Cell Cycle 12:21, 3390–3404; November 1, 2013; © 2013 Landes Bioscience

Stem cell-like ALDH^{bright} cellular states in EGFR-mutant non-small cell lung cancer

A novel mechanism of acquired resistance to erlotinib targetable with the natural polyphenol silibinin

Bruna Corominas-Faja[1,2,†], Cristina Oliveras-Ferraros[1,2,†], Elisabet Cuyàs[1,2], Antonio Segura-Carretero[3], Jorge Joven[4], Begoña Martin-Castillo[2,5], Enrique Barrajón-Catalán[6,7], Vicente Micol[6,7], Joaquim Bosch-Barrera[2,8], and Javier A Menendez[2,3,*]

[1]Metabolism & Cancer Group; Translational Research Laboratory; Catalan Institute of Oncology; Girona, Catalonia, Spain; [2]Girona Biomedical Research Institute (IDIBGI); Girona, Catalonia, Spain; [3]Department of Analytical Chemistry; Faculty of Sciences; University of Granada; Granada, Spain; [4]Unitat de Recerca Biomèdica (URB-CRB); Institut d'Investigació Sanitaria Pere i Virgili (IISPV); Universitat Rovira i Virgili; Reus, Catalonia, Spain; [5]Clinical Research Unit; Catalan Institute of Oncology; Girona, Catalonia, Spain; [6]Molecular and Cellular Biology Institute (IBMC); Miguel Hernández University; Elche, Alicante, Spain; [7]Monteloeder, Inc.; Elche, Alicante, Spain; [8]Medical Oncology; Catalan Institute of Oncology; Girona, Catalonia, Spain

[†]These authors contributed equally to work.

Keywords: silibinin, EGFR, erlotinib, cancer stem cells, lung cancer, ALDEFLUOR®

The enrichment of cancer stem cell (CSC)-like cellular states has not previously been considered to be a causative mechanism in the generalized progression of EGFR-mutant non-small cell lung carcinomas (NSCLC) after an initial response to the EGFR tyrosine kinase inhibitor erlotinib. To explore this possibility, we utilized a pre-clinical model of acquired erlotinib resistance established by growing NSCLC cells containing a TKI-sensitizing *EGFR* exon 19 deletion (Δ*E746-A750*) in the continuous presence of high doses of erlotinib. Genome-wide analyses using Agilent 44K Whole Human Genome Arrays were evaluated via bioinformatics analyses through GSEA-based screening of the KEGG pathway database to identify the molecular circuitries that were over-represented in the transcriptomic signatures of erlotinib-refractory cells. The genomic spaces related to erlotinib resistance included a preponderance of cell cycle genes (*E2F1*, *-2*, *CDC2*, *-6*) and DNA replication-related genes (*MCM4*, *-5*, *-6*, *-7*), most of which are associated with early lung development and poor prognosis. In addition, metabolic genes such as *ALDH1A3* (a candidate marker for lung cancer cells with CSC-like properties) were identified. Thus, we measured the proportion of erlotinib-resistant cells expressing very high levels of aldehyde dehydrogenase (ALDH) activity attributed to *ALDH1/3* isoforms. Using flow cytometry and the ALDEFLUOR® reagent, we confirmed that erlotinib-refractory cell populations contained drastically higher percentages (>4500%) of ALDH^{bright} cells than the parental erlotinib-responsive cells. Notably, strong decreases in the percentages of ALDH^{bright} cells were observed following incubation with silibinin, a bioactive flavonolignan that can circumvent erlotinib resistance in vivo. The number of lung cancer spheres was drastically suppressed by silibinin in a dose-dependent manner, thus confirming the ability of this agent to inhibit the self-renewal of erlotinib-refractory CSC-like cells. This report is the first to show that: (1) loss of responsiveness to erlotinib in EGFR-mutant NSCLC can be explained in terms of erlotinib-refractory ALDH^{bright} cells, which have been shown to exhibit stem cell-like properties; and (2) erlotinib-refractory ALDH^{bright} cells are sensitive to the natural agent silibinin. Our findings highlight the benefit of administration of silibinin in combination with EGFR TKIs to target CSCs and minimize the ability of tumor cells to escape cell death in EGFR-mutant NSCLC patients.

Introduction

Unlike other human carcinomas that originate from epithelial tissues, such as the intestine, mammary gland, and skin, relatively little has been elucidated regarding the role of so-called cancer stem cells (CSCs) in the response of non-small cell lung carcinomas (NSCLCs) to targeted therapies, which have revolutionized the treatment of NSCLCs over the past 10 y. One such targeted therapy is erlotinib, a small-molecule inhibitor of the intracellular tyrosine kinase activity of the epidermal growth factor receptor (EGFR). Erlotinib has been approved as a second-line therapy for advanced NSCLC in many countries.[1-5] Recent studies have revealed that erlotinib is highly efficacious in NSCLC patients with activating EGFR mutations, such as the Δ*E746-A750* exon 19 deletion and the *L858R* amino acid substitution.[6-10] Accordingly, patients with EGFR mutant advanced NSCLC

*Correspondence to: Javier A Menendez; Email: jmenendez@iconcologia.net, jmenendez@idibgi.org
Submitted: 08/26/2013; Accepted: 09/07/2013
http://dx.doi.org/10.4161/cc.26417

who receive first-line treatment with erlotinib have significantly longer progression-free survival (up to 14 mo), a 27-mo median survival rate, and fewer side effects than patients treated with traditional cytotoxic chemotherapy.[6-10] These findings validate the paradigm that the use of genomics-based approaches to stratify patients and determine an appropriate first-line targeted therapy can have direct applications and clinical impact. However, we should acknowledge that the efficacy of erlotinib monotherapy as a second-line treatment for advanced NSCLC is limited due to the low response rate (8.9%), brief duration of disease control, and minimal survival advantage.[1,3] Moreover, NSCLC patients with EGFR activating mutations who initially respond to erlotinib invariably develop acquired resistance through a variety of mechanisms and pathways.

Primary and acquired (secondary) resistance to erlotinib can occur through several distinct molecular mechanisms,[11-17] including the emergence of malignant clones containing second-site mutations in the EGFR kinase domain that abrogate the inhibitory activity of EGFR TKI (e.g., the so-called "gatekeeper mutation", which involves a substitution of methionine for threonine at position 790 [*T790M*]). Other molecular mechanisms include the acquisition of activating mutations downstream of EGFR (e.g., *K-Ras* or *PI3K*), amplification of the *MET* receptor tyrosine kinase (RTK) gene, or loss of the tumor suppressor gene *PTEN*. Recent evidence has suggested that additional mechanisms, including the activation of an epithelial-to-mesenchymal transition (EMT) phenomenon and the histological conversion from NSCLC to small cell lung cancer (SCLC), may also significantly contribute to erlotinib resistance in EGFR-mutant NSCLC.[18-29] The generation of CSC-like features through aberrant activation of the EMT genetic program[30-40] and increases in the CSC-like cell population are well known to be potential causes of the highly malignant activity and drug-refractoriness of SCLC in comparison with NSCLC.[41-45] However, studies addressing the possibility that subpopulations of NSCLC cells enriched with tumorigenic capacity and characterized by a specific stem cell-associated gene expression signature could explain the mechanism by which EGFR-mutant NSCLCs eventually stop responding to erlotinib have not yet been reported. In this scenario, we envision that: (1) the enrichment of CSC-like cellular states might play a causative role in the generalized progression of EGFR-mutant NSCLC after an initial response to erlotinib; and (2) novel treatments could be designed to eliminate erlotinib-refractory CSCs by inhibiting the maintenance of the stem-cell state. To explore these hypotheses, we utilized a preclinical model of acquired resistance to erlotinib established by growing PC-9 NSCLC cells containing a TKI-sensitizing *EGFR* exon 19 deletion (Δ*E746-A750*) in the continuous presence of high doses of erlotinib for several months. Using this model, which was developed in our laboratory,[46] we found that in the absence of second-site *EGFR* mutations, alternative activation of MET, AXL, or HER2, gain of secondary mutations in the *KRAS, NRAS*, or *BRAF* genes, or loss of the mutant *delE746-A750 EGFR* gene itself, the sole mechanism that accounted for the acquired resistance to erlotinib was a significant enrichment in EMT feature.[46,47] Here, we report for the first time an erlotinib-resistance transcriptomic signature that strongly suggests that erlotinib resistance can be explained by the acquisition of enhanced stem cell-like properties in EGFR-mutant NSCLC cell populations. Our study also demonstrates that erlotinib-refractory CSC cellular states, defined by the presence of very high levels of aldehyde dehydrogenase (ALDH) activity (i.e., $ALDH^{bright}$ cells), are exquisitely sensitive to the natural polyphenolic flavonoid silibinin, the active ingredient in milk thistle extracts that also exhibits anti-lung cancer activity.[47-51]

Results

Characterization of a pathway-based transcriptomic signature to predict the molecular function of the EGFR TKI erlotinib in EGFR-mutant NSCLC cells

To determine the effects specifically related to erlotinib efficacy in EGFR-mutant NSCLC cells, we performed genome-wide analyses by comparing the global transcriptomic profiles of erlotinib-sensitive PC-9 parental cells to those obtained in 2 pooled populations of erlotinib-refractory PC-9 derivatives (PC-9/Erl-R POOL1 and PC-9/Erl-R POOL2) following exposure to a clinically relevant dose of erlotinib. After RNA hybridization to an Agilent 44K (double density) Whole Human Genome Oligo Microarray (containing 45 220 probes representing 41 000 unique human genes and transcripts), normalized and filtered data from all experimental groups were simultaneously analyzed using the SAM algorithm. Using a 2.0-fold change cut-off value relative to the transcriptome of untreated erlotinib-sensitive PC-9 parental cells, genes that showed significant expression changes were identified. Only genes with well-annotated transcripts (not partial *cds* for hypothetical proteins, hypothetical insert cDNA clones, etc.) were selected, and genes that could not be identified were eliminated. We identified 297 and 247 genes that were differentially expressed in PC-9/Erl-R POOL1 and PC-9/Erl-R POOL2 cells, respectively. We then investigated the 155 overlapping genes (40%) obtained in both PC-9/Erl-R POOLs. **Table 1** summarizes up- and downregulated gene transcripts in the overlapping "erlotinib-resistance transcriptomic signature".

To identify functions that were significantly altered under selective pressure (i.e., erlotinib treatment), we used an experimental approach that was focused on gene pathways. Although several computational methods for incorporating biological pathway information and gene sets into microarray data analysis have been proposed, we decided to employ gene set enrichment analysis (GSEA), which determines whether an a priori defined set of genes shows statistically significant concordant differences between 2 biological states (e.g., erlotinib responsiveness and erlotinib refractoriness in EGFR-mutant NSCLC). We therefore applied GSEA (v2.0, http://www.broad.mit.edu/gsea/), an algorithm that is oriented to identify sets of functionally related genes and is widely used in the analysis of microarray data and over-representation analysis using Fisher exact test. As previously mentioned, we began by selecting a set of erlotinib-regulated genes that were differentially expressed in erlotinib-naïve and erlotinib-resistant tumor cells using the same number of gene sets

(i.e., 212) that were compiled from the Kyoto Encyclopedia of Genes and Genomes (KEGG) source in both analyses. Thus, GSEA was initially employed to perform a competitive pathway analysis of predefined gene sets in the transcriptomic signature obtained in erlotinib-treated PC-9 parental cells vs. erlotinib-treated Erl-R POOL1 and erlotinib-treated Erl-R POOL2. GSEA ranked all genes that were identified by expression arrays according to their differential expression between the 2 categories of samples. For each predefined gene set analyzed, the GSEA algorithm calculated a pathway enrichment score that indicated the extent to which the gene set was enriched for the highest or lowest ranking genes. Enrichment of the interesting genes within all available KEGG pathways that contained genes present on the microarray platform were tested with Fisher exact test, and pathways with q-values (FDR) of <5.0% were considered to be significantly enriched. We found that only 3 enriched gene sets, namely "DNA replication/mismatch repair", "cell cycle", and "lysine degradation/pyruvate metabolism", accounted for the differential molecular functions of erlotinib in erlotinib-sensitive PC-9 cells and PC-9 derivatives with acquired resistance to erlotinib (**Fig. 1**). Thus, the genomic spaces related to erlotinib resistance included a preponderance of "cell cycle" genes (e.g., *E2F1*, *-2*, *CDC2*, *-6*), "DNA replication"-related genes (e.g., *MCM4*, *-5*, *-6*, *-7*), and "metabolism" genes (e.g., *ALDH1A3*).

Because the majority of the gene families that were overrepresented in the erlotinib-resistance transcriptomic signature were associated with early lung development, poor prognosis, and stem cell-like properties,[52-64] we employed Ingenuity Pathway Analysis (IPA) using Ingenuity® software to confirm that the gene networks significantly associated with erlotinib resistance were directly related to stem cell biology and developmental processes. We utilized the "core analysis" function included in the software package to interpret erlotinib resistance-related global transcriptomic profiles in the context of biological processes, networks, and pathways. The IPA software algorithmically generates networks of up- and downregulated functionally related annotated genes based on their connectivity and assigns a score (i.e., a numerical value that considers both the number of focus genes in a network and the size of the network to approximate the relevance of each network in relation to the original list of focus genes). **Figure 2** graphically illustrates the two gene network functions that were most significantly (score ³3) upregulated (red) and downregulated (green) within the erlotinib resistance-related transcriptomic signature of EGFR-mutant NSCLC cells.

EGFR-mutant NSCLC cell populations with acquired resistance to erlotinib are enriched in ALDH^{bright} CSC-like cellular states

The genomic spaces that were significantly altered in erlotinib-refractory cells included overexpression of the *ALDH1A3* gene. *ALDH1A3* is a biomarker that has been suggested to label the tumorigenic cell fraction capable of self-renewal and tumor generation by recapitulating the heterogeneity of parental tumors (i.e., the CSCs), including NSCLCs.[65-69] In several types of tumors, cell subpopulations that are enriched for cancer-initiating activity have been readily identified by flow cytometry analysis using the ALDEFLUOR® reagent to identify cells with high levels of ALDH activity; these cells are thus referred to as ALDH^{bright} cells. The ALDEFLUOR® assay quantifies

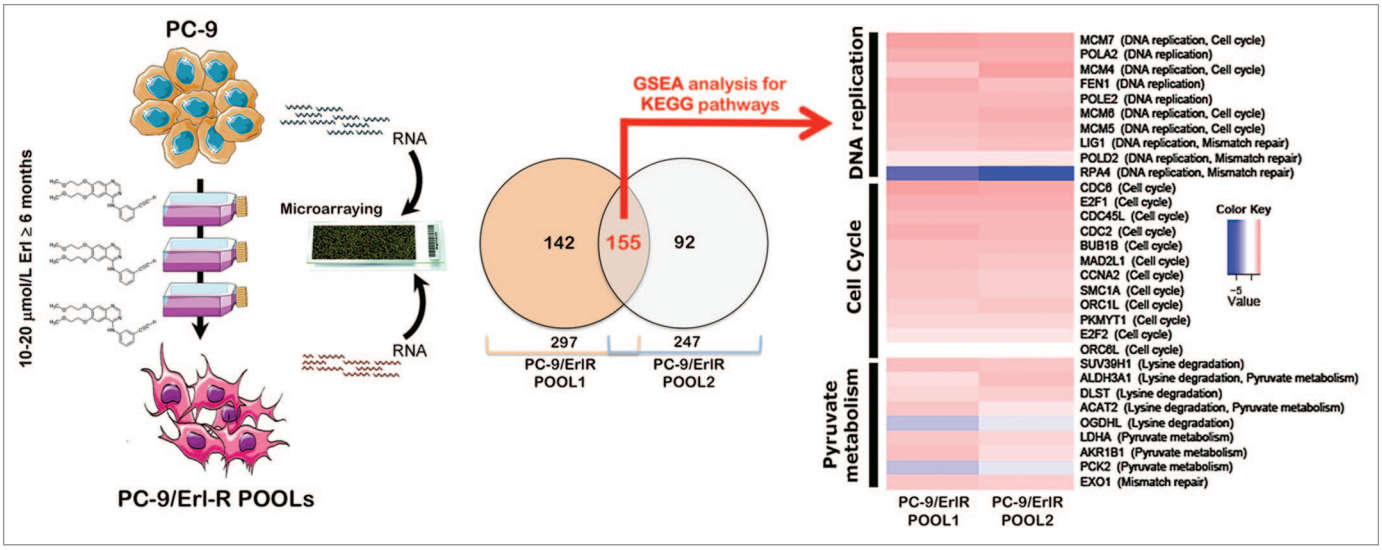

Figure 1. Pathway-based transcriptomic signature defining the erlotinib molecular function in EGFR-mutant NSCLC cells. Left. A schematic depicting the experimental approach designed to establish erlotinib-refractory populations (pools) of EGFR-mutant PC-9 NSCLC cells. Middle. The Venn diagram shows the overlap of genes whose expression was significantly altered following the acquisition of resistance to erlotinib. RNA was extracted from PC-9/Erl-R POOL1, PC-9/Erl-R POOL2, and PC-9 parental cells cultured in the presence of 1 µmol/L erlotinib. The RNA was then hybridized to G4112F Agilent Human Whole Genome Microarrays, and gene expression was analyzed as described in the "Materials and Methods" section. For the complete gene data, see **Table 1**. Right: The evolution of predictive biomarkers for erlotinib resistance in EGFR-mutant NSCLC cells was monitored using a pathway-based association analysis of genome-wide screening data as described in the "Materials and Methods" section. The heat map shows the clustered list of genes according to significant functions detected by GSEA with KEGG pathways. (1) DNA replication/mismatch repair; (2) Cell cycle; (3) Lysine degradation/pyruvate metabolism. The expression values are represented as colors, where the range of colors (red, pink, light blue, and dark blue) indicates the range of expression values (high, moderate, low, and lowest, respectively). Erl, erlotinib.

ALDH activity by measuring the conversion of the ALDH substrate BODIPY aminoacetaldehyde to the fluorescent product BODIPY aminoacetate. Addition of the inhibitor DEAB reduces ALDH-dependent fluorescence, thus confirming the correct identification of ALDH^{bright} cells. Because the ability to identify ALDH^{bright} cells by flow cytometry facilitates efforts to develop therapeutic approaches to target CSCs and elicit long-term and effective responses in cancer patients, we sought to determine whether erlotinib resistance in EGFR-mutant NSCLCs can be explained in terms of erlotinib-refractory ALDH^{bright} cells.

Using flow cytometry and the ALDEFLUOR® reagent to measure the proportion of erlotinib-resistant cells expressing high levels of ALDH activity (due to expression of ALDH1/3 isoforms), we confirmed that erlotinib-refractory cell populations contained drastically higher percentages of ALDH^{bright} cells than the parental erlotinib-responsive cells (**Fig. 3**). To identify ALDH^{bright} cells, a control aliquot (+ DEAB) of erlotinib-sensitive PC-9 cells was analyzed by flow cytometry, and the parameters were established to detect only the brightest of the ALDH-positive cells. Using this cut-off, the content of ALDH^{bright} cells was analyzed in the test (no DEAB) aliquot. In erlotinib-naïve PC-9 parental cells, approximately 0.2% of the cells expressed high ALDH activity. However, in erlotinib-refractory PC-9/Erl-R pooled populations, approximately 7% of the cells were ALDH^{bright}; therefore, the ALDH^{bright} cell content in erlotinib-refractory PC-9/Erl-R cells increased more than 4500-fold compared with erlotinib-responsive PC-9 parental cells.

The natural agent silibinin eliminates erlotinib-resistant ALDH^{bright} cells

We explored whether the flavonolignan silibinin, the only available experimental therapeutic that can circumvent erlotinib resistance in vivo,[47,48] can sensitize erlotinib-refractory ALDH^{bright} cells to erlotinib treatment. To evaluate the effects of silibinin on the proportion of ALDH^{bright} cells compared with vehicle treatment, erlotinib-refractory PC-9/Erl-R cells were treated (48 h) with increasing concentrations (50 and 100 μg/mL) of a milk thistle extract formulation that was enriched (30% *w/w*) with a water-soluble form of silibinin in complex with the amino-sugar

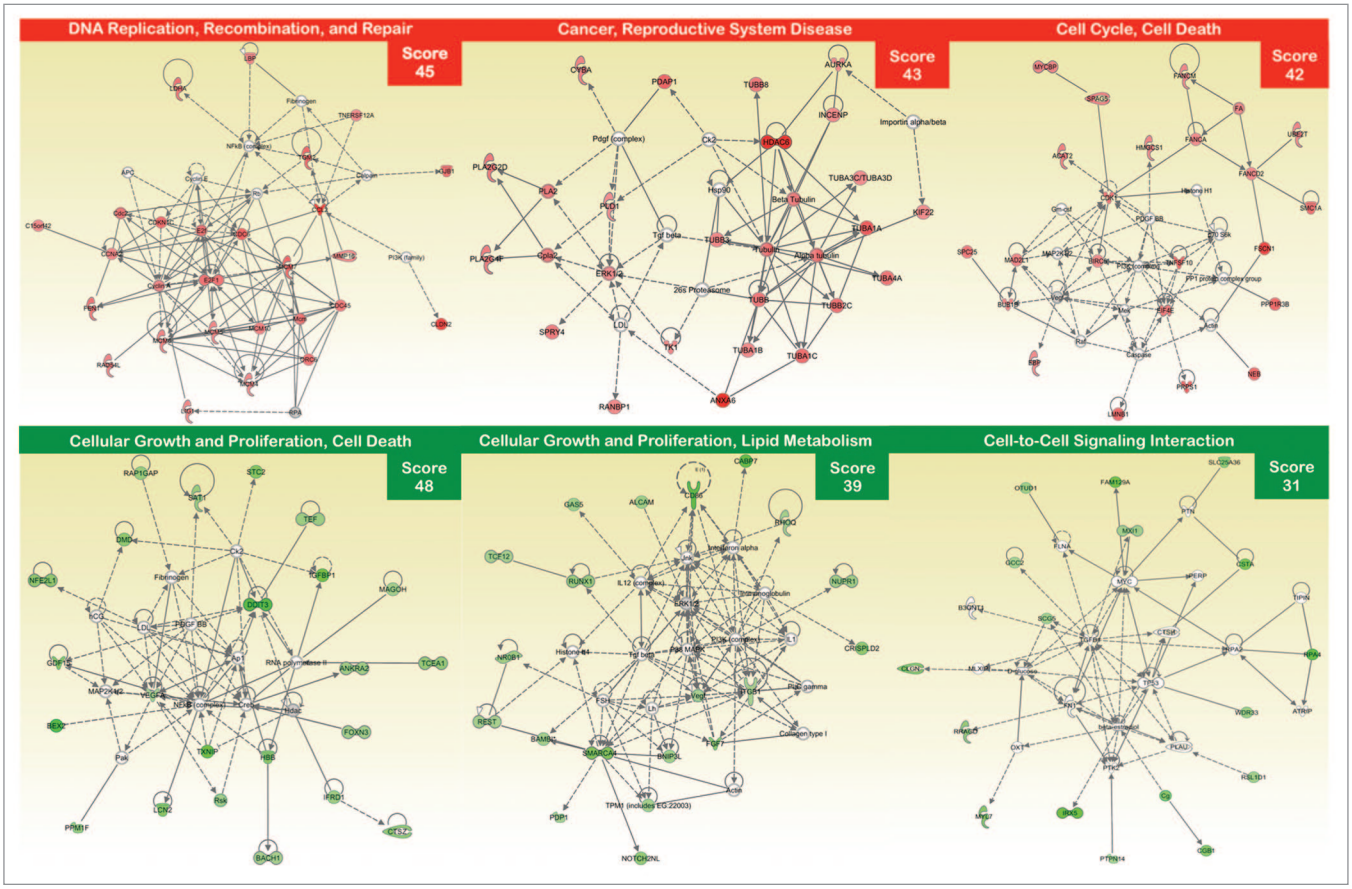

Figure 2. Network analysis of differentially expressed genes in EGFR-mutant PC-9 NSCLC cells that have acquired resistance to erlotinib. A data set containing the differentially expressed genes in response to erlotinib treatment (called the focus molecules, $n = 155$) between erlotinib-responsive PC-9 parental cells and erlotinib-refractory PC-9/Erl-R pools was overlaid onto a global molecular network developed from information contained in the Ingenuity Pathway (IPA) Knowledge Base. Networks of these focus molecules were then algorithmically generated based on their connectivity. The figure shows up- and downregulated networks (upper and bottom panels, respectively) with the 3 highest IPA scores (a composite measure that indicates the statistical significance of the interconnection between the molecules depicted in the network). The focus molecules are colored according to the gene expression (fold change) value; red gene symbols indicate upregulation, and green gene symbols indicate downregulation. The nodes are displayed using various shapes that represent the functional class of the gene product. Edges with dashed lines indicate indirect interactions, while continuous lines represent direct interactions.

meglumine. Notably, exogenous supplementation with silibinin led to a dose-dependent decrease in the proportion of ALDH^{bright} cells in the PC-9/Erl-R cell population. Incubation with 100 μg/mL silibinin-meglumine drastically decreased the proportion of erlotinib-refractory ALDH^{bright} cells by ~80% (**Fig. 3**).

Silibinin synergistically interacts with erlotinib to eliminate tumor sphere formation under CSC-selective conditions

Finally, we assessed whether the ability of silibinin to eliminate erlotinib-resistant ALDH^{bright} cells affects any of the biological properties that are commonly associated with CSC-related cellular states. PC-9/Erl-R cells grown under stem cell-selective conditions (i.e., as tumor spheres under non-adherent conditions in a serum-free medium supplemented with growth factors) were treated with increasing concentrations of silibinin and assessed for their sphere-forming efficiency. Exogenous supplementation with silibinin resulted in a dose-dependent reduction in the total number of growing spheres compared with the untreated controls (**Fig. 3**). Furthermore, silibinin treatment almost completely prevented sphere formation at concentrations that eliminated erlotinib-resistant ALDH^{bright} cells. Importantly, this decrease in tumor sphere formation was not due to non-specific silibinin toxicity, as determined by MTT uptake upon treatment with the same range of silibinin concentrations (**Fig. 3**).

Discussion

To identify master genes and molecular mechanisms implicated in the acquisition of erlotinib resistance in NSCLC cells containing an erlotinib-sensitizing *EGFR* exon 19 deletion (Δ*E746-A750*), we used an integrated profiling study. This study involved genome-wide analyses of Agilent 44K Whole Human Genome arrays and bioinformatics analyses using a GSEA-based screening method and the KEGG pathway database. This annotation approach, which precisely links gene products to defined biochemical circuitries, led to the identification of a gene expression signature associated with erlotinib resistance in a molecular background that lacked most of the mechanisms of secondary resistance that have been described to date.[46,47] We now present proof-of-concept evidence that in the absence of second-site *EGFR* mutations, MET hyperactivation, *PI3KCA* mutation, or activation of AXL, the acquisition of secondary resistance to erlotinib in EGFR-mutant NSCLCs can occur through the enrichment of stem cell-like gene expression profiles.

The preponderance of "cell cycle" (*E2F1*, *-2*, *CDC2*, *-6*), "DNA replication"-related (*MCM4*, *-5*, *-6*, *-7*), and "metabolism" (*ALDH3A1*) genes in the genomic spaces that were specifically related to erlotinib resistance notably paralleled the

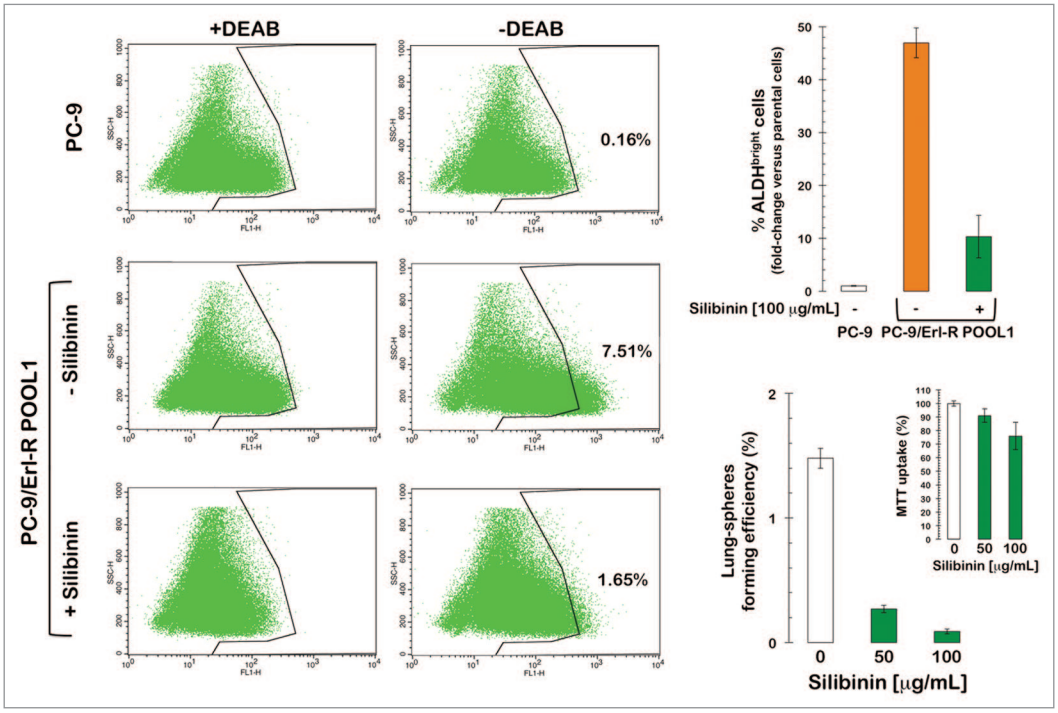

Figure 3. ALDH-expressing CSC-like cells in EGFR-mutant PC-9 NSCLC cells that have acquired resistance to erlotinib. Left: Erlotinib-naïve PC-9 parental cells and erlotinib-refractory PC-9/Erl-R cells were subjected to the ALDEFLUOR® assay to identify cells with high ALDH activity (ALDH^{bright}) in the absence or presence of silibinin. The ALDH inhibitor DEAB was used as a negative control. The cells without inhibitor shifted to the right and were considered ALDH^{bright} cells. Top right: The figure shows the fold change in the extension of the ALDH^{bright} subpopulation calculated by dividing the number of ALDH^{bright} cells in erlotinib-resistant PC-9/Erl-R cells (grown in the absence or presence of silibinin) by those in untreated PC-9 parental cells. Bottom right: TSFE of erlotinib-refractory PC-9/Erl-R cells in the absence or presence of increasing concentrations of silibinin was calculated as the number of spheres formed within 7 d divided by the original number of cells seeded. The results are expressed as percentages of the means (columns) ± SD (bars) (n = 2). Re-feeding of sphere cultures with silibinin and/or sphere medium was performed on days 3 and 5. The metabolic status of erlotinib-refractory PC-9/Erl-R cells treated with increasing concentrations of silibinin was measured using MTT uptake assays, and cell viability is expressed as % uptake relative to untreated control cells (= 100% cell viability). The results are presented as the mean (columns) ± SD (bars) of 2 independent experiments performed in triplicate.

Table 1. Gene transcripts differentially regulated in erlotinib-naïve PC-9 vs. erlotinib-refractory PC-9/ErlR POOL1 and PC-9/ErlR POOL1 cells cultured in the presence of erlotinib

Symbol	GENE NAME [ID]	ΔPool1	ΔPool2
BEX2	*Homo sapiens* brain expressed X–linked 2 (BEX2), mRNA [NM_032621]	–5,84	–3,55
THC2340803	Q6DD14 (Q6DD14) MGC80451 protein, partial (40%) [THC2340803]	–5,01	–10,86
BC054888	*Homo sapiens* cDNA clone MGC:61931 IMAGE:6565452, complete cds. [BC054888]	–4,84	–5,39
THC2317149	C40201 artifact-warning sequence (translated ALU class C) - human {*Homo sapiens*;}, partial (11%) [THC2317149]	–4,81	–10,12
DDIT3	*Homo sapiens* DNA–damage–inducible transcript 3 (DDIT3), mRNA [NM_004083]	–4,70	–3,21
CD86	*Homo sapiens* CD86 molecule (CD86), transcript variant 2, mRNA [NM_006889]	–4,37	–7,17
THC2281591	ALU5_HUMAN (P39192) Alu subfamily SC sequence contamination warning entry, partial (6%) [THC2281591]	–4,13	–7,30
RPA4	*Homo sapiens* replication protein A4, 34kDa (RPA4), mRNA [NM_013347]	–4,04	–7,85
CABP7	*Homo sapiens* calcium binding protein 7 (CABP7), mRNA [NM_182527]	–4,03	–8,99
N47124	N47124 yy53b06.r1 Soares_multiple_sclerosis_2NbHMSP *Homo sapiens* cDNA clone IMAGE:277235 5′, mRNA sequence [N47124]	–3,99	–8,45
LRRC2	*Homo sapiens* leucine rich repeat containing 2 (LRRC2), mRNA [NM_024512]	–3,98	–6,74
IRX5	*Homo sapiens* iroquois homeobox protein 5 (IRX5), mRNA [NM_005853]	–3,69	–6,67
STC2	*Homo sapiens* stanniocalcin 2 (STC2), mRNA [NM_003714]	–3,61	–2,09
TXNIP	*Homo sapiens* thioredoxin interacting protein (TXNIP), mRNA [NM_006472]	–3,58	–2,08
IGFBP1	*Homo sapiens* insulin-like growth factor binding protein 1 (IGFBP1), transcript variant 1, mRNA [NM_000596]	–3,52	–4,48
C1orf24	*Homo sapiens* chromosome 1 open reading frame 24 (C1orf24), transcript variant 2, mRNA [NM_052966]	–3,47	–2,08
RBM22	*Homo sapiens* RNA binding motif protein 22 (RBM22), mRNA [NM_018047]	–3,32	–6,78
CSTA	*Homo sapiens* cystatin A (stefin A) (CSTA), mRNA [NM_005213]	–3,20	–2,23
SAPS1	*Homo sapiens* SAPS domain family, member 1 (SAPS1), mRNA [NM_014931]	–3,09	–5,71
THC2286151	T09533 COX17 protein - human {*Homo sapiens*;}, partial (98%) [THC2286151]	–3,09	–6,09
SMARCA4	*Homo sapiens* SWI/SNF related, matrix associated, actin dependent regulator of chromatin, subfamily a, member 4 (SMARCA4), mRNA [NM_003072]	–3,05	–6,92
AA479896	zw44b06.s1 Soares_total_fetus_Nb2HF8_9w *Homo sapiens* cDNA clone IMAGE:772883 3′, mRNA sequence [AA479896]	–2,95	–6,41
CCDC66	*Homo sapiens* coiled–coil domain containing 66 (CCDC66), mRNA [NM_001012506]	–2,92	–7,33
LCN2	*Homo sapiens* lipocalin 2 (oncogene 24p3) (LCN2), mRNA [NM_005564]	–2,88	–2,42
CLGN	*Homo sapiens* calmegin (CLGN), mRNA [NM_004362]	–2,86	–2,03
AA704712	AA704712 zj21e01.s1 Soares_fetal_liver_spleen_1NFLS_S1 *Homo sapiens* cDNA clone IMAGE:450936 3′, mRNA sequence [AA704712]	–2,84	–6,61
TncRNA	*Homo sapiens* trophoblast–derived noncoding RNA (TncRNA) on chromosome 11 [NR_002802]	–2,82	–2,96
MYL7	*Homo sapiens* myosin, light polypeptide 7, regulatory (MYL7), mRNA [NM_021223]	–2,82	–2,90
BX119852	BX119852 Soares_testis_NHT *Homo sapiens* cDNA clone IMAGp998I221826 ; IMAGE:743517, mRNA sequence [BX119852]	–2,80	–5,84
CGB1	*Homo sapiens* chorionic gonadotropin, β polypeptide 1 (CGB1), mRNA [NM_033377]	–2,76	–6,79
THC2373518	Q6X1Z6 (Q6X1Z6) BICP22 transcription factor, partial (7%) [THC2373518]	–2,75	–6,34
S71486	dystrophin [human, Duchenne muscular dystrophy patient, mRNA Partial Mutant, 162 nt]. [S71486]	–2,71	–7,11
NFE2L1	*Homo sapiens* mRNA; cDNA DKFZp686K2237 (from clone DKFZp686K2237). [AL833530]	–2,67	–3,93
CRYAB	*Homo sapiens* crystallin, α B (CRYAB), mRNA [NM_001885]	–2,66	–2,71
CRISPLD2	*Homo sapiens* cysteine–rich secretory protein LCCL domain containing 2, mRNA (cDNA clone IMAGE:3953885), complete cds. [BC007689]	–2,64	–5,12

Table 1. Gene transcripts differentially regulated in erlotinib-naïve PC-9 vs. erlotinib-refractory PC-9/ErlR POOL1 and PC-9/ErlR POOL1 cells cultured in the presence of erlotinib (continued)

Symbol	GENE NAME [ID]	ΔPool1	ΔPool2
GRAMD1C	*Homo sapiens* GRAM domain containing 1C (GRAMD1C), mRNA [NM_017577]	−2,62	−5,56
SLC25A36	*Homo sapiens* solute carrier family 25, member 36 (SLC25A36), mRNA [NM_018155]	−2,61	−2,25
CTSZ	*Homo sapiens* cathepsin Z (CTSZ), mRNA [NM_001336]	−2,57	−3,09
NOTCH2NL	*Homo sapiens* Notch homolog 2 (*Drosophila*) N−terminal like (NOTCH2NL), mRNA [NM_203458]	−2,54	−2,15
ATF3	*Homo sapiens* activating transcription factor 3 (ATF3), transcript variant 2, mRNA [NM_004024]	−2,49	−2,82
VPS18	*Homo sapiens* vacuolar protein sorting protein 18 (VPS18), mRNA [NM_020857]	−2,48	−4,40
ZNF552	*Homo sapiens* cDNA FLJ13707 fis, clone PLACE2000347. [AK023769]	−2,46	−4,99
RRAGD	*Homo sapiens* Ras-related GTP binding D (RRAGD), mRNA [NM_021244]	−2,46	−2,47
ZCWPW1	*Homo sapiens* zinc finger, CW type with PWWP domain 1 (ZCWPW1), mRNA [NM_017984]	−2,45	−2,19
SAT	*Homo sapiens* spermidine/spermine N1-acetyltransferase (SAT), mRNA [NM_002970]	−2,43	−2,11
RAP1GAP	*Homo sapiens* RAP1 GTPase activating protein (RAP1GAP), mRNA [NM_002885]	−2,43	−5,07
THC2383841	ALU1_HUMAN (P39188) Alu subfamily J sequence contamination warning entry, partial (21%) [THC2383841]	−2,43	−4,69
RNF19	*Homo sapiens* ring finger protein 19 (RNF19), transcript variant 1, mRNA [NM_183419]	−2,42	−2,40
C6orf61	*Homo sapiens* cDNA FLJ20170 fis, clone COL09549. [AK000177]	−2,41	−2,54
MGC39584	*Homo sapiens* hypothetical gene supported by BC029568, mRNA (cDNA clone IMAGE:4838327), complete cds. [BC029568]	−2,41	−5,26
PPM1F	*Homo sapiens* protein phosphatase 1F (PP2C domain containing) (PPM1F), mRNA [NM_014634]	−2,36	−5,89
TEF	*Homo sapiens* thyrotrophic embryonic factor (TEF), mRNA [NM_003216]	−2,32	−3,96
LOC153222	*Homo sapiens* adult retina protein (LOC153222), mRNA [NM_153607]	−2,28	−2,19
IFRD1	*Homo sapiens* interferon−related developmental regulator 1 (IFRD1), transcript variant 2, mRNA [NM_001007245]	−2,27	−2,07
WDR33	*Homo sapiens* WD repeat domain 33 (WDR33), transcript variant 1, mRNA [NM_018383]	−2,22	−5,00
RNF150	*Homo sapiens* ring finger protein 150 (RNF150), mRNA [NM_020724]	−2,22	−4,21
OTUD1	*Homo sapiens* mRNA, clone: TH020D07. [AB188491]	−2,22	−2,25
ANKRA2	*Homo sapiens* ankyrin repeat, family A (RFXANK-like), 2 (ANKRA2), mRNA [NM_023039]	−2,19	−2,02
BNIP3L	*Homo sapiens* BCL2/adenovirus E1B 19kDa interacting protein 3-like (BNIP3L), mRNA [NM_004331]	−2,17	−2,04
RRAGC	*Homo sapiens* Ras−related GTP binding C (RRAGC), mRNA [NM_022157]	−2,17	−2,24
RHOQ	*Homo sapiens* ras homolog gene family, member Q (RHOQ), mRNA [NM_012249]	−2,12	−2,05
CHES1	*Homo sapiens* checkpoint suppressor 1 (CHES1), mRNA [NM_005197]	−2,11	−2,09
LOC286272	*Homo sapiens* cDNA FLJ10077 fis, clone HEMBA1001864. [AK000939]	−2,11	−3,56
CARD14	*Homo sapiens* mRNA; cDNA DKFZp667D139 (from clone DKFZp667D139). [AL833696]	−2,09	−2,33
AK094175	*Homo sapiens* cDNA FLJ36856 fis, clone ASTRO2014863. [AK094175]	−2,09	−2,81
FLJ32679	*Homo sapiens* golgin-like hypothetical protein LOC440321 (FLJ32679), mRNA [NM_001012452]	−2,08	−4,22
C8orf39	*Homo sapiens* PRO1905 mRNA, complete cds. [AF116672]	−2,08	−2,14
KIAA1407	*Homo sapiens* KIAA1407 (KIAA1407), mRNA [NM_020817]	−2,05	−2,22
FLJ10404	*Homo sapiens* hypothetical protein FLJ10404 (FLJ10404), mRNA [NM_019057]	−2,03	−3,64
GCC2	*Homo sapiens* GRIP and coiled−coil domain containing 2 (GCC2), transcript variant 1, mRNA [NM_181453]	−2,02	−3,23
LPXN	*Homo sapiens* leupaxin (LPXN), mRNA [NM_004811]	−2,02	−2,44

Table 1. Gene transcripts differentially regulated in erlotinib-naïve PC-9 vs. erlotinib-refractory PC-9/ErlR POOL1 and PC-9/ErlR POOL1 cells cultured in the presence of erlotinib (continued)

Symbol	GENE NAME [ID]	ΔPool1	ΔPool2
PPM2C	*Homo sapiens* protein phosphatase 2C, magnesium–dependent, catalytic subunit (PPM2C), nuclear gene encoding mitochondrial protein, mRNA [NM_018444]	−2,01	−2,09
RRM2	*Homo sapiens* ribonucleotide reductase M2 polypeptide (RRM2), mRNA [NM_001034]	2,02	2,07
DKK4	*Homo sapiens* dickkopf homolog 4 (*Xenopus laevis*) (DKK4), mRNA [NM_014420]	2,03	2,17
FANCD2	*Homo sapiens* Fanconi anemia, complementation group D2 (FANCD2), transcript variant 2, mRNA [NM_001018115]	2,04	2,06
SHCBP1	*Homo sapiens* SHC SH2–domain binding protein 1 (SHCBP1), mRNA [NM_024745]	2,04	2,08
NOC2L	*Homo sapiens* nucleolar complex associated 2 homolog (*S. cerevisiae*) (NOC2L), mRNA [NM_015658]	2,05	2,16
TOMM40	*Homo sapiens* translocase of outer mitochondrial membrane 40 homolog (yeast) (TOMM40), mRNA [NM_006114]	2,05	2,16
INCENP	*Homo sapiens* inner centromere protein antigens 135/155kDa (INCENP), transcript variant 2, mRNA [NM_020238]	2,07	2,08
MCM4	*Homo sapiens* MCM4 minichromosome maintenance deficient 4 (*S. cerevisiae*) (MCM4), transcript variant 1, mRNA [NM_005914]	2,07	2,66
AI608782	AI608782 tw94 g05.x1 NCI_CGAP_HN6 *Homo sapiens* cDNA clone IMAGE:2267384 3′ similar to gb:K00558 TUBULIN ALPHA-1 CHAIN (HUMAN);, mRNA sequence [AI608782]	2,08	2,14
LIG1	*Homo sapiens* ligase I, DNA, ATP-dependent (LIG1), mRNA [NM_000234]	2,09	2,11
TK1	*Homo sapiens* thymidine kinase 1, soluble (TK1), mRNA [NM_003258]	2,09	2,00
POLD2	*Homo sapiens* polymerase (DNA directed), delta 2, regulatory subunit 50kDa (POLD2), mRNA [NM_006230]	2,10	2,12
TUBB3	*Homo sapiens* tubulin, β 3 (TUBB3), mRNA [NM_006086]	2,11	2,01
THC2308747	Q969M7 (Q969M7) NEDD8-conjugating enzyme NCE2, partial (70%) [THC2308747]	2,11	2,07
MAD2L1	*Homo sapiens* MAD2 mitotic arrest deficient-like 1 (yeast) (MAD2L1), mRNA [NM_002358]	2,11	2,01
HIST1H3D	*Homo sapiens* histone 1, H3d (HIST1H3D), mRNA [NM_003530]	2,12	2,08
BUB1B	*Homo sapiens* BUB1 budding uninhibited by benzimidazoles 1 homolog β (yeast) (BUB1B), mRNA [NM_001211]	2,12	2,18
MYCBP	*Homo sapiens* c-myc binding protein (MYCBP), mRNA [NM_012333]	2,13	2,31
MCM5	*Homo sapiens* MCM5 minichromosome maintenance deficient 5, cell division cycle 46 (*S. cerevisiae*) (MCM5), mRNA [NM_006739]	2,13	2,28
LOC285986	*Homo sapiens* cDNA FLJ39130 fis, clone NTONG2007756. [AK096449]	2,15	2,22
NT5DC2	*Homo sapiens* 5′-nucleotidase domain containing 2 (NT5DC2), mRNA [NM_022908]	2,16	2,28
RAD54L	*Homo sapiens* RAD54-like (*S. cerevisiae*) (RAD54L), mRNA [NM_003579]	2,16	2,05
HNRPAB	*Homo sapiens* heterogeneous nuclear ribonucleoprotein A/B (HNRPAB), transcript variant 2, mRNA [NM_004499]	2,16	2,07
PRPS1L1	*Homo sapiens* phosphoribosyl pyrophosphate synthetase 1-like 1 (PRPS1L1), mRNA [NM_175886]	2,18	2,06
TRIP13	*Homo sapiens* thyroid hormone receptor interactor 13 (TRIP13), mRNA [NM_004237]	2,18	2,05
USP5	*Homo sapiens* ubiquitin specific peptidase 5 (isopeptidase T) (USP5), mRNA [NM_003481]	2,18	2,24
C1orf100	*Homo sapiens* chromosome 1 open reading frame 100 (C1orf100), mRNA [NM_001012970]	2,19	2,06
TUBA2	*Homo sapiens* tubulin, α 2 (TUBA2), transcript variant 2, mRNA [NM_079836]	2,19	2,10
SPAG5	*Homo sapiens* sperm associated antigen 5 (SPAG5), mRNA [NM_006461]	2,20	2,02
MCM10	*Homo sapiens* MCM10 minichromosome maintenance deficient 10 (*S. cerevisiae*) (MCM10), transcript variant 1, mRNA [NM_182751]	2,21	2,16
ZWINT	*Homo sapiens* ZW10 interactor (ZWINT), transcript variant 4, mRNA [NM_001005414]	2,22	2,15
SUV39H1	*Homo sapiens* suppressor of variegation 3–9 homolog 1 (*Drosophila*) (SUV39H1), mRNA [NM_003173]	2,22	2,07

Table 1. Gene transcripts differentially regulated in erlotinib-naïve PC-9 vs. erlotinib-refractory PC-9/ErlR POOL1 and PC-9/ErlR POOL1 cells cultured in the presence of erlotinib (continued)

Symbol	GENE NAME [ID]	ΔPool1	ΔPool2
THAP9	*Homo sapiens* THAP domain containing 9 (THAP9), mRNA [NM_024672]	2,23	2,28
KPNA2	*Homo sapiens* karyopherin α 2 (RAG cohort 1, importin α 1) (KPNA2), mRNA [NM_002266]	2,23	2,00
MCM6	*Homo sapiens* MCM6 minichromosome maintenance deficient 6 (MIS5 homolog, S. pombe) (*S. cerevisiae*) (MCM6), mRNA [NM_005915]	2,23	2,38
RDH12	*Homo sapiens* retinol dehydrogenase 12 (all-trans/9-cis/11-cis) (RDH12), mRNA [NM_152443]	2,25	2,07
LOC442013	PREDICTED: *Homo sapiens* similar to L-lactate dehydrogenase A chain (LDH–A) (LDH muscle subunit) (LDH-M) (Proliferation-inducing gene 19 protein) (LOC442013), mRNA [XM_941152]	2,27	2,22
AK027315	*Homo sapiens* cDNA FLJ14409 fis, clone HEMBA1004408, moderately similar to PEPTIDYL-PROLYL CIS-TRANS ISOMERASE 10 (EC 5.2.1.8). [AK027315]	2,31	2,10
FKBP4	*Homo sapiens* FK506 binding protein 4, 59kDa (FKBP4), mRNA [NM_002014]	2,31	2,11
POLE2	*Homo sapiens* polymerase (DNA directed), epsilon 2 (p59 subunit) (POLE2), mRNA [NM_002692]	2,32	2,31
TUBB8	*Homo sapiens* tubulin, β 8 (TUBB8), mRNA [NM_177987]	2,32	2,26
CDC45L	*Homo sapiens* CDC45 cell division cycle 45-like (*S. cerevisiae*) (CDC45L), mRNA [NM_003504]	2,34	2,31
SPBC25	*Homo sapiens* spindle pole body component 25 homolog (*S. cerevisiae*) (SPBC25), mRNA [NM_020675]	2,35	2,11
PNMA2	*Homo sapiens* paraneoplastic antigen MA2 (PNMA2), mRNA [NM_007257]	2,36	2,26
TUBB	*Homo sapiens* tubulin, β (TUBB), mRNA [NM_178014]	2,37	2,23
RHOV	*Homo sapiens* ras homolog gene family, member V (RHOV), mRNA [NM_133639]	2,39	2,19
CDC2	*Homo sapiens* cell division cycle 2, G_1 to S and G_2 to M (CDC2), transcript variant 1, mRNA [NM_001786]	2,39	2,26
SNRPB	*Homo sapiens* small nuclear ribonucleoprotein polypeptides B and B1 (SNRPB), transcript variant 1, mRNA [NM_198216]	2,40	2,18
FLJ38020	*Homo sapiens* similar to absent in melanoma 1 (FLJ38020), mRNA [NM_001039775]	2,40	2,19
TUBA1	*Homo sapiens* tubulin, α 1 (testis specific) (TUBA1), mRNA [NM_006000]	2,40	2,21
ORC6L	*Homo sapiens* origin recognition complex, subunit 6 like (yeast) (ORC6L), mRNA [NM_014321]	2,41	2,28
MVK	*Homo sapiens* mevalonate kinase (mevalonic aciduria) (MVK), mRNA [NM_000431]	2,42	2,03
SNRP70	*Homo sapiens* small nuclear ribonucleoprotein 70kDa polypeptide (RNP antigen) (SNRP70), transcript variant 1, mRNA [NM_003089]	2,43	2,18
FEN1	*Homo sapiens* flap structure-specific endonuclease 1 (FEN1), mRNA [NM_004111]	2,44	2,22
TMEM149	*Homo sapiens* transmembrane protein 149 (TMEM149), mRNA [NM_024660]	2,46	2,16
E2F1	*Homo sapiens* E2F transcription factor 1 (E2F1), mRNA [NM_005225]	2,47	2,40
LOC554207	*Homo sapiens* hypothetical LOC554207, mRNA (cDNA clone MGC:21504 IMAGE:3882600), complete cds. [BC031469]	2,47	2,11
POLA2	*Homo sapiens* polymerase (DNA directed), α 2 (70kD subunit) (POLA2), mRNA [NM_002689]	2,49	2,49
TUBB2C	*Homo sapiens* tubulin, β 2C (TUBB2C), mRNA [NM_006088]	2,49	2,34
LDHA	*Homo sapiens* lactate dehydrogenase A (LDHA), mRNA [NM_005566]	2,49	2,42
GINS2	*Homo sapiens* GINS complex subunit 2 (Psf2 homolog) (GINS2), mRNA [NM_016095]	2,49	2,57
KIAA1199	*Homo sapiens* KIAA1199 (KIAA1199), mRNA [NM_018689]	2,50	3,17
SMC1A	*Homo sapiens* structural maintenance of chromosomes 1A (SMC1A), mRNA [NM_006306]	2,51	2,33
GJB1	*Homo sapiens* gap junction protein, β 1, 32kDa (connexin 32, Charcot-Marie-Tooth neuropathy, X-linked) (GJB1), mRNA [NM_000166]	2,51	2,14
NEB	*Homo sapiens* nebulin (NEB), mRNA [NM_004543]	2,52	2,11
AW952039	AW952039 EST364109 MAGE resequences, MAGB *Homo sapiens* cDNA, mRNA sequence [AW952039]	2,55	2,66
LMNB1	*Homo sapiens* lamin B1 (LMNB1), mRNA [NM_005573]	2,56	2,52

Table 1. Gene transcripts differentially regulated in erlotinib-naïve PC-9 vs. erlotinib-refractory PC-9/ErlR POOL1 and PC-9/ErlR POOL1 cells cultured in the presence of erlotinib (continued)

Symbol	GENE NAME [ID]	ΔPool1	ΔPool2
TUBA6	*Homo sapiens* tubulin, α 6 (TUBA6), mRNA [NM_032704]	2,56	2,47
BQ184185	BQ184185 UI-E-EJ1-ajs-i-07-0-UI.s1 UI-E-EJ1 *Homo sapiens* cDNA clone UI-E-EJ1-ajs-i-07-0-UI 3′, mRNA sequence [BQ184185]	2,58	2,55
ACOX2	*Homo sapiens* acyl-Coenzyme A oxidase 2, branched chain (ACOX2), mRNA [NM_003500]	2,59	2,82
PPP1R3B	*Homo sapiens* protein phosphatase 1, regulatory (inhibitor) subunit 3B (PPP1R3B), mRNA [NM_024607]	2,61	2,16
SRGAP2	*Homo sapiens* SLIT-ROBO Rho GTPase activating protein 2 (SRGAP2), mRNA [NM_015326]	2,65	2,34
AK074346	*Homo sapiens* cDNA FLJ23766 fis, clone HEP19192. [AK074346]	2,67	2,45
PRPS1	*Homo sapiens* phosphoribosyl pyrophosphate synthetase 1 (PRPS1), mRNA [NM_002764]	2,72	2,75
PDAP1	*Homo sapiens* PDGFA associated protein 1 (PDAP1), mRNA [NM_014891]	2,73	2,80
MCM7	*Homo sapiens* MCM7 minichromosome maintenance deficient 7 (*S. cerevisiae*) (MCM7), transcript variant 2, mRNA [NM_182776]	2,73	2,53
CDC6	*Homo sapiens* CDC6 cell division cycle 6 homolog (*S. cerevisiae*) (CDC6), mRNA [NM_001254]	2,77	2,63
TUBA3	*Homo sapiens* tubulin, α 3 (TUBA3), mRNA [NM_006009]	2,88	2,67
ENST00000299997	*Homo sapiens* hypothetical protein MGC9913, mRNA (cDNA clone IMAGE:3870821), complete cds. [BC008651]	2,89	2,73
CLDN2	*Homo sapiens* claudin 2 (CLDN2), mRNA [NM_020384]	3,32	2,33
CCL2	*Homo sapiens* chemokine (C-C motif) ligand 2 (CCL2), mRNA [NM_002982]	3,53	2,24
FGFBP1	*Homo sapiens* fibroblast growth factor binding protein 1 (FGFBP1), mRNA [NM_005130]	3,60	2,03
ANXA6	*Homo sapiens* annexin A6 (ANXA6), transcript variant 1, mRNA [NM_001155]	3,80	3,28

appearance of erlotinib-refractory ALDH^{bright} cells, which have been shown to exhibit many of the properties attributed to CSCs in NSCLC (including tumorigenicity in immunodeficient mice). The intracellular family of ALDH enzymes participates in cellular detoxification, differentiation, and drug resistance through the oxidation of cellular aldehydes. The ALDEFLUOR® assay was developed by the successful isolation of viable hematopoietic stem cells from human umbilical cord blood and was reported to be specific for ALDH1A, the ALDH isoform found in high abundance in these cells. However, while individual ALDH isoforms do display some preferred substrate specificity, the isoforms also exhibit cross-reactivity; therefore, the ALDEFLUOR® assay likely detects the ALDH activity of one or more ALDH isoforms expressed in these cells. In this regard, the ALDEFLUOR®-based detection of ALDH activity in breast CSCs has recently been reported to be primarily due to ALDH1A3 expression.[70] Two aldehyde dehydrogenase isozymes, ALDH1A1 and ALDH3A1, are expressed in putative lung epithelial stem cell niches, overexpressed in tumors compared with normal lung, and overexpressed in NSCLCs compared with small cell lung cancers (SCLCs). Jiang et al.[69] originally found that ALDH selected for stem-like tumor cells in 2 NSCLC cell lines, and observed that ALDH1 expression was associated with poor survival in a cohort of stage 1 NSCLC patients. Although we did not directly assess the expression status of ALDH1 isoforms in sorted erlotinib-refractory ALDH^{bright} cells, the suggestion that the higher levels of ALDH1A3 mRNA in erlotinib-refractory cells compared with erlotinib-responsive parental cells contributed to the enhanced ALDEFLUOR® activity is reasonable.

During the preparation of this manuscript, Shien et al.[71] similarly reported that acquired resistance to the EGFR inhibitor gefitinib is associated with a manifestation of stem cell-like properties in NSCLC cells, including EMT features, overexpression of ALDH1A1, increase in side-population, and self-renewal capacity. These authors reported that clinically applicable HDAC inhibitors (such as trichostatin A and vorinostat) and a proteasome inhibitor (bortezomib) exhibited similar antitumor efficacy against both parental and resistant cells. However, the authors did not investigate whether the sensitivity of gefitinib-refractory NSCLC cells to HDAC and proteasome inhibitors was related to the ability of these agents to suppress stem cell-like properties in NSCLC cells with acquired resistance to gefitinib.[71] Our study demonstrates that erlotinib-refractory ALDH^{bright} cells are sensitive to the natural polyphenol silibinin, a putative chemo-preventive agent that has been shown to efficiently suppress tumor growth in primary and acquired erlotinib-resistant NSCLC cells.[47,48] Wang et al.[72] have demonstrated that silibinin inhibits colon CSC-like self-renewal and sphere formation by suppressing the PP2A/AKT/mTOR pathway, suggesting that silibinin may be a useful compound for the development of new strategies to modulate CSCs in cancer therapy. We have recently discovered that silibinin fully reverses the EMT-related high miR-21/low miR-200c microRNA signature and represses the expression of the mesenchymal markers SNAIL, ZEB, and N-cadherin observed in erlotinib-refractory

NSCLC tumors in vivo.[47] In accordance with the CSC theory, the elimination of CSC cellular states should be the critical criterion used to define the efficacy of a therapy, rather than measuring only reductions in tumor volume. Given that complete abrogation of tumor growth was observed in erlotinib-refractory NSCLC xenografts following co-administration of erlotinib and silibinin, our current findings suggest that silibinin primarily affects cancer stem/progenitor cells (rather than differentiated cancer cell populations). These results definitively highlight the benefits that co-administration of silibinin and erlotinib may offer in targeting CSCs and minimizing the potential of tumor cells to escape death in EGFR-mutant NSCLC patients. We have recently described the rapid activation of a mesenchymal-like phenotype upon treatment with erlotinib alone in NSCLCs harboring the erlotinib-sensitizing EGFR exon 19 mutation Δ*E746-A750*.[46] This observation provides a putative mechanism underlying the emergence of stem cell-like properties in NSCLC cells continuously exposed to high concentrations of erlotinib. Erlotinib-based therapeutic protocols can prevent tumor cell death, and the inhibition of ALDH activity has been suggested as a potential strategy to eliminate CSCs and overcome drug resistance; thus, the ability of silibinin to impede the EMT genetic program,[73] activate the reciprocal mesenchymal-to-epithelial transition (MET), and prevent the highly migratory phenotype of erlotinib-resistant mesenchymal NSCLC cells strongly highlights the potential benefit of combining silibinin and erlotinib therapies to minimize these effects in NSCLC patients who initially respond to erlotinib.

Silibinin is known to display poor water solubility. However, the ionization capacity of silibinin increases upon combination with the excipient amino sugar meglumine, which is highly water-soluble. In the current study and those demonstrating the ability of silibinin to fully restore drug sensitivity to EGFR-mutant NSCLC xenografts with EMT-driven resistance to erlotinib, we employed a milk thistle extract that was rich in silibinin-meglumine (a commercially used water-soluble formulation of silibinin). If the systemic bioavailability of silibinin-meglumine is improved to allow higher bioactive concentrations of silibinin in vivo, the combination of erlotinib and silibinin may serve as an effective intervention to limit the enrichment of erlotinib-refractory CSC-like cellular states. If this possibility is achieved, ALDH activity and tumor sphere formation may serve as biomarkers in clinical studies aimed to prevent resistance to erlotinib treatment. Future trials with pharmacokinetic, pharmacodynamics, and toxicity endpoints after treatment with water-soluble silibinin-meglumine are urgently needed. If proven safe and effective, the administration of the naturally occurring flavonolignan silibinin could become an acceptable non-toxic long-term strategy to prevent the manifestation of stem cell-like ALDH^{bright} cellular states, which is a novel mechanism by which EGFR-mutant NSCLC patients can develop resistance to erlotinib.

Materials and Methods

Drugs and chemicals

The EGFR (HER1) TKI erlotinib (Tarceva®) was a kind gift from Roche Pharmaceuticals. Stock solutions of erlotinib were prepared at 10 mmol/L in DMSO and stored in aliquots in the dark at –20°C until utilization. The water-soluble milk thistle extract was provided by Monteloeder, SL in its silibinin-meglumine salt form (Elche). For the experiments, all drug solutions were prepared fresh from stock solutions and diluted with cell growth medium. The control cells were cultured in media containing identical concentrations (v/v) of vehicle.

Cell line

PC-9 NSCLC-derived cells expressing the EGFR exon 19 deletion mutation (*delE746-A750*) were obtained from the IBL cell bank (Gunma).

Generation of PC-9 cells with acquired resistance to erlotinib

To establish EGFR-mutant NSCLC cells with acquired resistance to erlotinib, cultures of PC-9 NSCLC cells were continuously exposed to high doses of erlotinib (1 μmol/L) in routine culture medium, which was replaced every 1–2 d for approximately 2 mo. Initially, the PC-9 cell numbers were substantially reduced, and for the next 3 mo, the surviving cells were passaged in the presence of up to 20 μmol/L erlotinib approximately every 10–12 d at a seeding ratio of 1:2. The cell proliferation rates slowly increased over the next 2 mo, allowing passaging every 5–7 d at a seeding ratio of 1:5. A stable growth rate was reached after a total of 6 mo, and routine maintenance of the PC-9/Erl-R (erlotinib-resistant) pooled populations involved passage every 5 d at a seeding ratio of 1:10 of the confluent cell culture grown in the presence of 10 μmol/L erlotinib.

Agilent gene chip analyses

Total RNA isolated from erlotinib-sensitive PC-9 parental cells and 2 pooled populations of erlotinib-refractory PC-9 cells (i.e., Erl-R POOL1 and Erl-R POOL2) grown in the presence of erlotinib was isolated with TRIzol reagent (Invitrogen) according to the manufacturer's instructions. The RNA quantity and quality were determined using the RNA 6000 Nano Assay kit on an Agilent 2100 BioAnalyzer (Agilent Technologies) as recommended. Agilent Human Whole Genome Microarrays (G4112F) containing 45 220 probes were then hybridized. Briefly, 500 ng of total RNA from each sample was amplified by Oligo-dT-T7 reverse transcription and labeled by in vitro transcription with T7 RNA polymerase in the presence of Cy5-CTP or Cy3-CTP using the Quick Amp Labeling Kit (Agilent) and purified using RNeasy columns (Qiagen). After fragmentation, 825 ng of labeled cRNA from each of the 2 samples was co-hybridized in in situ hybridization buffer (Agilent) for 17 h at 65 °C and washed at room temperature (RT) for 1 min in Gene Expression Wash Buffer 1 (Agilent) and 1 min at 37 °C in Gene Expression Wash Buffer 2 (Agilent).

Statistical analysis of microarray data

The images were generated on a confocal microarray scanner (G2565BA, Agilent) at 5 μm resolution and quantified using GenePix 6.0 software (Molecular Dynamics). Spots with signal intensities that were twice that of the local background, not saturated, and not flagged by GenePix were considered reliable. Extracted intensities were background-corrected, and the log2 ratios were normalized in an intensity-dependent fashion by the global LOWESS method (intra-chip normalization). Normalized log2 ratios were scaled between arrays to allow

comparisons between all data. The raw data were processed using MMARGE, a web implementation of Limma (a microarray analysis library developed within the Bioconductor project in the R statistical environment). To identify genes that were differentially expressed, the multiclass SAM (significance analysis of microarrays) procedure was applied. Probes with *Q* values (FDR) below 5% and fold changes exceeding 2.0 in absolute value were initially selected as the relevant spots. The microarray probes were collapsed to genes by considering the median log2 ratio of the respective probes per gene.

Functional analysis of microarray data

GSEA was applied to gain additional insight into the biological context of the genes that were differentially regulated. GSEA is a computational method that determines whether an a priori defined set of genes shows statistically significant and/or concordant differences between 2 biological states (e.g., phenotypes). The combination of genes commonly regulated between the 2 data sets was then used to generate a list of interesting genes. Enrichment of the interesting genes within all available (i.e., 212) KEGG pathways that contain genes present on the microarray platform were tested using Fisher exact test. Pathways with *Q* values (FDR) <5% were considered to be significantly enriched.

Ingenuity analysis

Gene networks were constructed using Ingenuity Pathway Analysis (Ingenuity® Systems). Data sets containing identifiers of genes that were >2.0-fold up- or downregulated were uploaded into the application. These "focus genes" were overlaid onto a global molecular network developed from information contained in the Ingenuity Pathway Knowledge Base. Networks of these "focus genes" (nodes) were algorithmically generated based on the principle that highly connected gene networks are the most biologically meaningful networks. All edges were supported by at least one reference from the literature stored in the Ingenuity Pathway Knowledge Base (the IPA interaction database is manually curated by scientists and updated quarterly). Briefly, the user-input or "focus genes" list was compared with the "global molecular network" (GMN) database, consisting of thousands of genes and interactions. The focus genes were sorted based on highest to lowest connectivity within the GMN, and networks of approximately 35 genes were grown starting with the most connected focus gene. IPA assigns a *P* value for a network of size *n* and an input focus gene list of size *f* by calculating the probability of finding *f* or more focus genes in a randomly selected set of *n* genes from the GMN. The intensity of the node color indicated the degree of expression (green scale for downregulated nodes; red scale for upregulated nodes). The nodes were displayed using various shapes, each of which represents a functional class of the gene products. The score indicated the likelihood of the genes in a network being found together due to random chance. Using a 99% confidence interval, scores of ≥3 were significant.

ALDEFLUOR® activity assay

The ALDEFLUOR® kit (Stem Cell Technologies) was used to profile cells with high and low ALDH activity. Briefly, cells were suspended in ALDEFLUOR® assay buffer containing the fluorescent ALDH substrate BODIPY-aminoacetaldehyde (BAAA) and incubated for 45 min at 37 °C. The assay buffer also contained a transport inhibitor to prevent efflux of BAAA from the cells. BAAA passively diffuses into live cells and is then converted by intracellular ALDH into a negatively charged product (BODIPY-aminoacetate) that is retained inside cells, labeling the cells with a bright fluorescent signal. After a washing step, the brightly fluorescent ALDH-expressing cells ($ALDH^{bright}$) were detected in the green fluorescence channel (FL1; 520–540 nm) on a FACSCalibur instrument (BD Biosciences). A sample of cells was further stained with a specific ALDH inhibitor, diethylaminobenzaldehyde (DEAB) (Sigma), to serve as a negative control for each experiment. Because only cells with an intact cellular membrane can retain the ALDH1 reaction product, only viable $ALDH^{bright}$ cells were identified. Cells incubated with BAAA and DEAB were used to establish the background signal and define the $ALDH^{bright}$ region. Incubation of cells with the substrate in the absence of DEAB induced a shift in the BAAA fluorescence and defined the $ALDH^{bright}$ population.

Tumor sphere cultures

Lung cancer spheres were generated from single PC-9/Erl-R POOL1 cells seeded at 10^3 cells/cm^2 in 6-well ultralow attachment plates (Corning Inc). Sphere medium (F-12/DMEM containing 5 mg/mL insulin, 0.5 mg/mL hydrocortisone, 2% B27, and 20 ng/mL epidermal growth factor) was prepared as originally described by Dontu et al.[74] in the absence or presence of increasing concentrations of silibinin. Tumor sphere-forming efficiency (TSFE) was calculated as the number of sphere-like structures formed within 7 d divided by the original number of cells seeded and expressed as a percentage of the mean (± SD).

Cell viability assays

The effect of silibinin on cell viability was determined using a standard colorimetric MTT (3–4, 5-dimethylthiazol-2-yl-2, 5-diphenyltetrazolium bromide) reduction assay. For each treatment, the cell viability was evaluated as a percentage using the following equation: (OD_{570} of the treated sample/OD_{570} of the untreated sample) × 100.

Statistics

Two-group comparisons were performed using the Student *t* test for paired and unpaired values. Comparisons of means of ³3 groups were performed by ANOVA, and the existence of individual differences (in cases with significant F values by ANOVA) were tested by Scheffé multiple comparisons. In all cases, the statistical analyses were performed using XLSTAT (Addinsoft™), and $P < 0.01$ was considered to be significant.

Disclosure of Potential Conflicts of Interest

No potential conflicts of interest were disclosed.

Acknowledgments

This work was supported by a charity collection organized by the Fundació Roses Contra el Cáncer (Roses, Girona, Catalonia). This work was also financially supported by the Instituto de Salud Carlos III (Ministerio de Sanidad y Consumo, Fondo de Investigación Sanitaria (FIS), Spain, grants CP05-00090, PI06-0778 and RD06-0020-0028), the Fundación Científica de la Asociación Española Contra el Cáncer (AECC, Spain), and

the Ministerio de Ciencia e Innovación (SAF2009-11579 and SAF2012-38914, Plan Nacional de I+D+ I, MICINN, Spain). Alejandro Vazquez-Martin received a Sara Borrell post-doctoral contract (CD08/00283, Ministerio de Sanidad y Consumo, Fondo de Investigación Sanitaria -FIS-, Spain). Sílvia Cufí received a research fellowship (Formación de Personal Investigador, FPI) from the Ministerio de Ciencia e Innovación (MICINN, Spain). This work was also supported by grants AGL2011-29857-C03-03 (MICINN, Spain), PROMETEO/2012/007 and ACOMP/2013/093 (Generalitat Valenciana), and CIBER (CB12/03/30038, Fisiopatología de la Obesidad y la Nutrición, CIBERobn, Instituto de Salud Carlos III).

References

1. Passaro A, Cortesi E, de Marinis F. Second-line treatment of non-small-cell lung cancer: chemotherapy or tyrosine kinase inhibitors? Expert Rev Anticancer Ther 2011; 11:1587-97; PMID:21999132; http://dx.doi.org/10.1586/era.11.120
2. Natale RB, Thongprasert S, Greco FA, Thomas M, Tsai CM, Sunpaweravong P, Ferry D, Mulatero C, Whorf R, Thompson J, et al. Phase III trial of vandetanib compared with erlotinib in patients with previously treated advanced non-small-cell lung cancer. J Clin Oncol 2011; 29:1059-66; PMID:21282542; http://dx.doi.org/10.1200/JCO.2010.28.5981
3. Shepherd FA, Rodrigues Pereira J, Ciuleanu T, Tan EH, Hirsh V, Thongprasert S, Campos D, Maoleekoonpiroj S, Smylie M, Martins R, et al.; National Cancer Institute of Canada Clinical Trials Group. Erlotinib in previously treated non-small-cell lung cancer. N Engl J Med 2005; 353:123-32; PMID:16014882; http://dx.doi.org/10.1056/NEJMoa050753
4. Ciuleanu T, Stelmakh L, Cicenas S, Miliauskas S, Grigorescu AC, Hillenbach C, Johannsdottir HK, Klughammer B, Gonzalez EE. Efficacy and safety of erlotinib versus chemotherapy in second-line treatment of patients with advanced, non-small-cell lung cancer with poor prognosis (TITAN): a randomised multicentre, open-label, phase 3 study. Lancet Oncol 2012; 13:300-8; PMID:22277837; http://dx.doi.org/10.1016/S1470-2045(11)70385-0
5. Qi WX, Tang LN, He AN, Shen Z, Lin F, Yao Y. Erlotinib and pemetrexed as maintenance therapy for advanced non-small-cell lung cancer: a systematic review and indirect comparison. Curr Med Res Opin 2012; 28:643-50; PMID:22414178; http://dx.doi.org/10.1185/03007995.2012.675880
6. Rosell R, Moran T, Queralt C, Porta R, Cardenal F, Camps C, Majem M, Lopez-Vivanco G, Isla D, Provencio M, et al.; Spanish Lung Cancer Group. Screening for epidermal growth factor receptor mutations in lung cancer. N Engl J Med 2009; 361:958-67; PMID:19692684; http://dx.doi.org/10.1056/NEJMoa0904554
7. Rosell R, Moran T, Cardenal F, Porta R, Viteri S, Molina MA, Benlloch S, Taron M. Predictive biomarkers in the management of EGFR mutant lung cancer. Ann N Y Acad Sci 2010; 1210:45-52; PMID:20973798; http://dx.doi.org/10.1111/j.1749-6632.2010.05775.x
8. Rosell R, Morán T, Carcereny E, Quiroga V, Molina MA, Costa C, Benlloch S, Tarón M. Non-small-cell lung cancer harbouring mutations in the EGFR kinase domain. Clin Transl Oncol 2010; 12:75-80; PMID:20156777; http://dx.doi.org/10.1007/S12094-010-0473-0
9. Rosell R, Carcereny E, Gervais R, Vergnenegre A, Massuti B, Felip E, Palmero R, Garcia-Gomez R, Pallares C, Sanchez JM, et al.; Spanish Lung Cancer Group in collaboration with Groupe Français de Pneumo-Cancérologie and Associazione Italiana Oncologia Toracica. Erlotinib versus standard chemotherapy as first-line treatment for European patients with advanced EGFR mutation-positive non-small-cell lung cancer (EURTAC): a multicentre, open-label, randomised phase 3 trial. Lancet Oncol 2012; 13:239-46; PMID:22285168; http://dx.doi.org/10.1016/S1470-2045(11)70393-X
10. Santarpia M, De Pas TM, Altavilla G, Spaggiari L, Rosell R. Moving towards molecular-guided treatments: erlotinib and clinical outcomes in non-small-cell lung cancer patients. Future Oncol 2013; 9:327-45; PMID:23469969; http://dx.doi.org/10.2217/fon.13.6
11. Morgillo F, Bareschino MA, Bianco R, Tortora G, Ciardiello F. Primary and acquired resistance to anti-EGFR targeted drugs in cancer therapy. Differentiation 2007; 75:788-99; PMID:17608727; http://dx.doi.org/10.1111/j.1432-0436.2007.00200.x
12. Nguyen KS, Kobayashi S, Costa DB. Acquired resistance to epidermal growth factor receptor tyrosine kinase inhibitors in non-small-cell lung cancers dependent on the epidermal growth factor receptor pathway. Clin Lung Cancer 2009; 10:281-9; PMID:19632948; http://dx.doi.org/10.3816/CLC.2009.n.039
13. Gazdar AF. Activating and resistance mutations of EGFR in non-small-cell lung cancer: role in clinical response to EGFR tyrosine kinase inhibitors. Oncogene 2009; 28(Suppl 1):S24-31; PMID:19680293; http://dx.doi.org/10.1038/onc.2009.198
14. Xu Y, Liu H, Chen J, Zhou Q. Acquired resistance of lung adenocarcinoma to EGFR-tyrosine kinase inhibitors gefitinib and erlotinib. Cancer Biol Ther 2010; 9:572-82; PMID:20404520; http://dx.doi.org/10.4161/cbt.9.8.11881
15. Ayoola A, Barochia A, Belani K, Belani CP. Primary and acquired resistance to epidermal growth factor receptor tyrosine kinase inhibitors in non-small cell lung cancer: an update. Cancer Invest 2012; 30:433-46; PMID:22571344; http://dx.doi.org/10.3109/07357907.2012.666691
16. Lin L, Bivona TG. Mechanisms of Resistance to Epidermal Growth Factor Receptor Inhibitors and Novel Therapeutic Strategies to Overcome Resistance in NSCLC Patients. Chemother Res Pract 2012; 2012:817297; PMID:22970367; http://dx.doi.org/10.1155/2012/817297
17. Nakata A, Gotoh N. Recent understanding of the molecular mechanisms for the efficacy and resistance of EGF receptor-specific tyrosine kinase inhibitors in non-small cell lung cancer. Expert Opin Ther Targets 2012; 16:771-81; PMID:22762482; http://dx.doi.org/10.1517/14728222.2012.697155
18. Sequist LV, Waltman BA, Dias-Santagata D, Digumarthy S, Turke AB, Fidias P, Bergethon K, Shaw AT, Gettinger S, Cosper AK, et al. Genotypic and histological evolution of lung cancers acquiring resistance to EGFR inhibitors. Sci Transl Med 2011; 3:75ra26; PMID:21430269; http://dx.doi.org/10.1126/scitranslmed.3002003
19. Thomson S, Buck E, Petti F, Griffin G, Brown E, Ramnarine N, Iwata KK, Gibson N, Haley JD. Epithelial to mesenchymal transition is a determinant of sensitivity of non-small-cell lung carcinoma cell lines and xenografts to epidermal growth factor receptor inhibition. Cancer Res 2005; 65:9455-62; PMID:16230409; http://dx.doi.org/10.1158/0008-5472.CAN-05-1058
20. Fuchs BC, Fujii T, Dorfman JD, Goodwin JM, Zhu AX, Lanuti M, Tanabe KK. Epithelial-to-mesenchymal transition and integrin-linked kinase mediate sensitivity to epidermal growth factor receptor inhibition in human hepatoma cells. Cancer Res 2008; 68:2391-9; PMID:18381447; http://dx.doi.org/10.1158/0008-5472.CAN-07-2460
21. Yauch RL, Januario T, Eberhard DA, Cavet G, Zhu W, Fu L, Pham TQ, Soriano R, Stinson J, Seshagiri S, et al. Epithelial versus mesenchymal phenotype determines in vitro sensitivity and predicts clinical activity of erlotinib in lung cancer patients. Clin Cancer Res 2005; 11:8686-98; PMID:16361555; http://dx.doi.org/10.1158/1078-0432.CCR-05-1492
22. Coldren CD, Helfrich BA, Witta SE, Sugita M, Lapadat R, Zeng C, Barón A, Franklin WA, Hirsch FR, Geraci MW, et al. Baseline gene expression predicts sensitivity to gefitinib in non-small cell lung cancer cell lines. Mol Cancer Res 2006; 4:521-8; PMID:16877703; http://dx.doi.org/10.1158/1541-7786.MCR-06-0095
23. Suda K, Tomizawa K, Fujii M, Murakami H, Osada H, Maehara Y, Yatabe Y, Sekido Y, Mitsudomi T. Epithelial to mesenchymal transition in an epidermal growth factor receptor-mutant lung cancer cell line with acquired resistance to erlotinib. J Thorac Oncol 2011; 6:1152-61; PMID:21597390; http://dx.doi.org/10.1097/JTO.0b013e318216ee52
24. Chung JH, Rho JK, Xu X, Lee JS, Yoon HI, Lee CT, Choi YJ, Kim HR, Kim CH, Lee JC. Clinical and molecular evidences of epithelial to mesenchymal transition in acquired resistance to EGFR-TKIs. Lung Cancer 2011; 73:176-82; PMID:21168239; http://dx.doi.org/10.1016/j.lungcan.2010.11.011
25. Chang TH, Tsai MF, Su KY, Wu SG, Huang CP, Yu SL, Yu YL, Lan CC, Yang CH, Lin SB, et al. Slug confers resistance to the epidermal growth factor receptor tyrosine kinase inhibitor. Am J Respir Crit Care Med 2011; 183:1071-9; PMID:21037017; http://dx.doi.org/10.1164/rccm.201009-1440OC
26. Bryant JL, Britson J, Balko JM, Willian M, Timmons R, Frolov A, Black EP. A microRNA gene expression signature predicts response to erlotinib in epithelial cancer cell lines and targets EMT. Br J Cancer 2012; 106:148-56; PMID:22045191; http://dx.doi.org/10.1038/bjc.2011.465
27. Zhang X, Liu G, Kang Y, Dong Z, Qian Q, Ma X. N-cadherin expression is associated with acquisition of EMT phenotype and with enhanced invasion in erlotinib-resistant lung cancer cell lines. PLoS One 2013; 8:e57692; PMID:23520479; http://dx.doi.org/10.1371/journal.pone.0057692
28. Zhang Z, Lee JC, Lin L, Olivas V, Au V, LaFramboise T, Abdel-Rahman M, Wang X, Levine AD, Rho JK, et al. Activation of the AXL kinase causes resistance to EGFR-targeted therapy in lung cancer. Nat Genet 2012; 44:852-60; PMID:22751098; http://dx.doi.org/10.1038/ng.2330
29. Byers LA, Diao L, Wang J, Saintigny P, Girard L, Peyton M, Shen L, Fan Y, Giri U, Tumula PK, et al. An epithelial–mesenchymal transition gene signature predicts resistance to EGFR and PI3K inhibitors and identifies Axl as a therapeutic target for overcoming EGFR inhibitor resistance. Clin Cancer Res 2013; 19:279-90; PMID:23091115; http://dx.doi.org/10.1158/1078-0432.CCR-12-1558
30. Ouyang G, Wang Z, Fang X, Liu J, Yang CJ. Molecular signaling of the epithelial to mesenchymal transition in generating and maintaining cancer stem cells. Cell Mol Life Sci 2010; 67:2605-18; PMID:20238234; http://dx.doi.org/10.1007/s00018-010-0338-2
31. Singh A, Settleman J. EMT, cancer stem cells and drug resistance: an emerging axis of evil in the war on cancer. Oncogene 2010; 29:4741-51; PMID:20531305; http://dx.doi.org/10.1038/onc.2010.215

32. Wang Z, Li Y, Ahmad A, Azmi AS, Kong D, Banerjee S, Sarkar FH. Targeting miRNAs involved in cancer stem cell and EMT regulation: An emerging concept in overcoming drug resistance. Drug Resist Updat 2010; 13:109-18; PMID:20692200; http://dx.doi.org/10.1016/j.drup.2010.07.001
33. Takebe N, Warren RQ, Ivy SP. Breast cancer growth and metastasis: interplay between cancer stem cells, embryonic signaling pathways and epithelial-to-mesenchymal transition. Breast Cancer Res 2011; 13:211; PMID:21672282; http://dx.doi.org/10.1186/bcr2876
34. Floor S, van Staveren WC, Larsimont D, Dumont JE, Maenhaut C. Cancer cells in epithelial-to-mesenchymal transition and tumor-propagating-cancer stem cells: distinct, overlapping or same populations. Oncogene 2011; 30:4609-21; PMID:21643013; http://dx.doi.org/10.1038/onc.2011.184
35. Nurwidya F, Takahashi F, Murakami A, Takahashi K. Epithelial mesenchymal transition in drug resistance and metastasis of lung cancer. Cancer Res Treat 2012; 44:151-6; PMID:23091440; http://dx.doi.org/10.4143/crt.2012.44.3.151
36. Scheel C, Weinberg RA. Cancer stem cells and epithelial–mesenchymal transition: concepts and molecular links. Semin Cancer Biol 2012; 22:396-403; PMID:22554795; http://dx.doi.org/10.1016/j.semcancer.2012.04.001
37. Bao B, Azmi AS, Ali S, Ahmad A, Li Y, Banerjee S, Kong D, Sarkar FH. The biological kinship of hypoxia with CSC and EMT and their relationship with deregulated expression of miRNAs and tumor aggressiveness. Biochim Biophys Acta 2012; 1826:272-96; PMID:22579961
38. Dave B, Mittal V, Tan NM, Chang JC. Epithelial–mesenchymal transition, cancer stem cells and treatment resistance. Breast Cancer Res 2012; 14:202; PMID:22264257; http://dx.doi.org/10.1186/bcr2938
39. Sato M, Shames DS, Hasegawa Y. Emerging evidence of epithelial-to-mesenchymal transition in lung carcinogenesis. Respirology 2012; 17:1048-59; PMID:22452538; http://dx.doi.org/10.1111/j.1440-1843.2012.02173.x
40. Shih JY, Yang PC. The EMT regulator slug and lung carcinogenesis. Carcinogenesis 2011; 32:1299-304; PMID:21665887; http://dx.doi.org/10.1093/carcin/bgr110
41. Qiu X, Wang Z, Li Y, Miao Y, Ren Y, Luan Y. Characterization of sphere-forming cells with stem-like properties from the small cell lung cancer cell line H446. Cancer Lett 2012; 323:161-70; PMID:22521544; http://dx.doi.org/10.1016/j.canlet.2012.04.004
42. Salcido CD, Larochelle A, Taylor BJ, Dunbar CE, Varticovski L. Molecular characterisation of side population cells with cancer stem cell-like characteristics in small-cell lung cancer. Br J Cancer 2010; 102:1636-44; PMID:20424609; http://dx.doi.org/10.1038/sj.bjc.6605668
43. Kubo T, Takigawa N, Osawa M, Harada D, Ninomiya T, Ochi N, Ichihara E, Yamane H, Tanimoto M, Kiura K. Subpopulation of small-cell lung cancer cells expressing CD133 and CD87 show resistance to chemotherapy. Cancer Sci 2013; 104:78-84; PMID:23066953; http://dx.doi.org/10.1111/cas.12045
44. Wang P, Gao Q, Suo Z, Munthe E, Solberg S, Ma L, Wang M, Westerdaal NA, Kvalheim G, Gaudernack G. Identification and characterization of cells with cancer stem cell properties in human primary lung cancer cell lines. PLoS One 2013; 8:e57020; PMID:23469181; http://dx.doi.org/10.1371/journal.pone.0057020
45. Zhang Z, Zhou Y, Qian H, Shao G, Lu X, Chen Q, Sun X, Chen D, Yin R, Zhu H, et al. Stemness and inducing differentiation of small cell lung cancer NCI-H446 cells. Cell Death Dis 2013; 4:e633; PMID:23681228; http://dx.doi.org/10.1038/cddis.2013.152
46. Vazquez-Martin A, Cufí S, Oliveras-Ferraros C, Torres-Garcia VZ, Corominas-Faja B, Cuyàs E, Bonavia R, Visa J, Martin-Castillo B, Barrajón-Catalán E, et al. IGF-1R/epithelial-to-mesenchymal transition (EMT) crosstalk suppresses the erlotinib-sensitizing effect of EGFR exon 19 deletion mutations. Sci Rep 2013; 3:2560; PMID:23994953; http://dx.doi.org/10.1038/srep02560
47. Cufí S, Bonavia R, Vazquez-Martin A, Oliveras-Ferraros C, Corominas-Faja B, Cuyàs E, Martin-Castillo B, Barrajón-Catalán E, Visa J, Segura-Carretero A, et al. Silibinin suppresses EMT-driven erlotinib resistance by reversing the high miR-21/low miR-200c signature in vivo. Sci Rep 2013; 3:2459; PMID:23963283; http://dx.doi.org/10.1038/srep02459
48. Rho JK, Choi YJ, Jeon BS, Choi SJ, Cheon GJ, Woo SK, Kim HR, Kim CH, Choi CM, Lee JC. Combined treatment with silibinin and epidermal growth factor receptor tyrosine kinase inhibitors overcomes drug resistance caused by T790M mutation. Mol Cancer Ther 2010; 9:3233-43; PMID:21159609; http://dx.doi.org/10.1158/1535-7163.MCT-10-0625
49. Mateen S, Raina K, Agarwal C, Chan D, Agarwal R. Silibinin synergizes with histone deacetylase and DNA methyltransferase inhibitors in upregulating E-cadherin expression together with inhibition of migration and invasion of human non-small cell lung cancer cells. J Pharmacol Exp Ther 2013; 345:206-14; PMID:23461975; http://dx.doi.org/10.1124/jpet.113.203471
50. Mateen S, Raina K, Agarwal R. Chemopreventive and anti-cancer efficacy of silibinin against growth and progression of lung cancer. Nutr Cancer 2013; 65(Suppl 1):3-11; PMID:23682778; http://dx.doi.org/10.1080/01635581.2013.785004
51. Sadava D, Kane SE. Silibinin reverses drug resistance in human small-cell lung carcinoma cells. Cancer Lett 2013; 339:102-6; PMID:23879966; http://dx.doi.org/10.1016/j.canlet.2013.07.017
52. Fujioka S, Shomori K, Nishihara K, Yamaga K, Nosaka K, Araki K, Haruki T, Taniguchi Y, Nakamura H, Ito H. Expression of minichromosome maintenance 7 (MCM7) in small lung adenocarcinomas (pT1): Prognostic implication. Lung Cancer 2009; 65:223-9; PMID:19144445; http://dx.doi.org/10.1016/j.lungcan.2008.11.007
53. Kikuchi J, Kinoshita I, Shimizu Y, Kikuchi E, Takeda K, Aburatani H, Oizumi S, Konishi J, Kaga K, Matsuno Y, et al. Minichromosome maintenance (MCM) protein 4 as a marker for proliferation and its clinical and clinicopathological significance in non-small cell lung cancer. Lung Cancer 2011; 72:229-37; PMID:20884074; http://dx.doi.org/10.1016/j.lungcan.2010.08.020
54. Toyokawa G, Masuda K, Daigo Y, Cho HS, Yoshimatsu M, Takawa M, Hayami S, Maejima K, Chino M, Field HI, et al. Minichromosome Maintenance Protein 7 is a potential therapeutic target in human cancer and a novel prognostic marker of non-small cell lung cancer. Mol Cancer 2011; 10:65; PMID:21619671; http://dx.doi.org/10.1186/1476-4598-10-65
55. Huang CL, Liu D, Nakano J, Yokomise H, Ueno M, Kadota K, Wada H. E2F1 overexpression correlates with thymidylate synthase and survivin gene expressions and tumor proliferation in non small-cell lung cancer. Clin Cancer Res 2007; 13:6938-46; PMID:18056168; http://dx.doi.org/10.1158/1078-0432.CCR-07-1539
56. Chong JL, Wenzel PL, Sáenz-Robles MT, Nair V, Ferrey A, Hagan JP, Gomez YM, Sharma N, Chen HZ, Ouseph M, et al. E2f1-3 switch from activators in progenitor cells to repressors in differentiating cells. Nature 2009; 462:930-4; PMID:20016602; http://dx.doi.org/10.1038/nature08677
57. Park YY, Park ES, Kim SB, Kim SC, Sohn BH, Chu IS, Jeong W, Mills GB, Byers LA, Lee JS. Development and validation of a prognostic gene-expression signature for lung adenocarcinoma. PLoS One 2012; 7:e44225; PMID:22970185; http://dx.doi.org/10.1371/journal.pone.0044225
58. Yu YH, Chiou GY, Huang PI, Lo WL, Wang CY, Lu KH, Yu CC, Alterovitz G, Huang WC, Lo JF, et al. Network biology of tumor stem-like cells identified a regulatory role of CBX5 in lung cancer. Sci Rep 2012; 2:584; PMID:22900142; http://dx.doi.org/10.1038/srep00584
59. Gonzalez S, Klatt P, Delgado S, Conde E, Lopez-Rios F, Sanchez-Cespedes M, Mendez J, Antequera F, Serrano M. Oncogenic activity of Cdc6 through repression of the INK4/ARF locus. Nature 2006; 440:702-6; PMID:16572177; http://dx.doi.org/10.1038/nature04585
60. Ucar D, Cogle CR, Zucali JR, Ostmark B, Scott EW, Zori R, Gray BA, Moreb JS. Aldehyde dehydrogenase activity as a functional marker for lung cancer. Chem Biol Interact 2009; 178:48-55; PMID:18952074; http://dx.doi.org/10.1016/j.cbi.2008.09.029
61. Moreb JS, Baker HV, Chang LJ, Amaya M, Lopez MC, Ostmark B, Chou W. ALDH isozymes down-regulation affects cell growth, cell motility and gene expression in lung cancer cells. Mol Cancer 2008; 7:87; PMID:19025616; http://dx.doi.org/10.1186/1476-4598-7-87
62. Sullivan JP, Spinola M, Dodge M, Raso MG, Behrens C, Gao B, Schuster K, Shao C, Larsen JE, Sullivan LA, et al. Aldehyde dehydrogenase activity selects for lung adenocarcinoma stem cells dependent on notch signaling. Cancer Res 2010; 70:9937-48; PMID:21118965; http://dx.doi.org/10.1158/0008-5472.CAN-10-0881
63. Liang D, Shi Y. Aldehyde dehydrogenase-1 is a specific marker for stem cells in human lung adenocarcinoma. Med Oncol 2012; 29:633-9; PMID:21484084; http://dx.doi.org/10.1007/s12032-011-9933-9
64. Huang CP, Tsai MF, Chang TH, Tang WC, Chen SY, Lai HH, Lin TY, Yang JC, Yang PC, Shih JY, et al. ALDH-positive lung cancer stem cells confer resistance to epidermal growth factor receptor tyrosine kinase inhibitors. Cancer Lett 2013; 328:144-51; PMID:22935675; http://dx.doi.org/10.1016/j.canlet.2012.08.021
65. Chute JP, Muramoto GG, Whitesides J, Colvin M, Safi R, Chao NJ, McDonnell DP. Inhibition of aldehyde dehydrogenase and retinoid signaling induces the expansion of human hematopoietic stem cells. Proc Natl Acad Sci U S A 2006; 103:11707-12; PMID:16857736; http://dx.doi.org/10.1073/pnas.0603806103
66. Cheung AM, Wan TS, Leung JC, Chan LY, Huang H, Kwong YL, Liang R, Leung AY. Aldehyde dehydrogenase activity in leukemic blasts defines a subgroup of acute myeloid leukemia with adverse prognosis and superior NOD/SCID engrafting potential. Leukemia 2007; 21:1423-30; PMID:17476279; http://dx.doi.org/10.1038/sj.leu.2404721
67. Pearce DJ, Taussig D, Simpson C, Allen K, Rohatiner AZ, Lister TA, Bonnet D. Characterization of cells with a high aldehyde dehydrogenase activity from cord blood and acute myeloid leukemia samples. Stem Cells 2005; 23:752-60; PMID:15917471; http://dx.doi.org/10.1634/stemcells.2004-0292

68. Patel M, Lu L, Zander DS, Sreerama L, Coco D, Moreb JS. ALDH1A1 and ALDH3A1 expression in lung cancers: correlation with histologic type and potential precursors. Lung Cancer 2008; 59:340-9; PMID:17920722; http://dx.doi.org/10.1016/j.lungcan.2007.08.033
69. Jiang F, Qiu Q, Khanna A, Todd NW, Deepak J, Xing L, Wang H, Liu Z, Su Y, Stass SA, et al. Aldehyde dehydrogenase 1 is a tumor stem cell-associated marker in lung cancer. Mol Cancer Res 2009; 7:330-8; PMID:19276181; http://dx.doi.org/10.1158/1541-7786.MCR-08-0393
70. Marcato P, Dean CA, Giacomantonio CA, Lee PW. Aldehyde dehydrogenase: its role as a cancer stem cell marker comes down to the specific isoform. Cell Cycle 2011; 10:1378-84; PMID:21552008; http://dx.doi.org/10.4161/cc.10.9.15486
71. Shien K, Toyooka S, Yamamoto H, Soh J, Jida M, Thu KL, Hashida S, Maki Y, Ichihara E, Asano H, et al. Acquired resistance to EGFR inhibitors is associated with a manifestation of stem cell-like properties in cancer cells. Cancer Res 2013; 73:3051-61; PMID:23542356; http://dx.doi.org/10.1158/0008-5472.CAN-12-4136
72. Wang JY, Chang CC, Chiang CC, Chen WM, Hung SC. Silibinin suppresses the maintenance of colorectal cancer stem-like cells by inhibiting PP2A/AKT/mTOR pathways. J Cell Biochem 2012; 113:1733-43; PMID:22213051
73. Cufí S, Bonavia R, Vazquez-Martin A, Corominas-Faja B, Oliveras-Ferraros C, Cuyàs E, Martin-Castillo B, Barrajón-Catalán E, Visa J, Segura-Carretero A, et al. Silibinin meglumine, a water-soluble form of milk thistle silymarin, is an orally active anti-cancer agent that impedes the epithelial-to-mesenchymal transition (EMT) in EGFR-mutant non-small-cell lung carcinoma cells. Food Chem Toxicol 2013; 60:360-8; PMID:23916468; http://dx.doi.org/10.1016/j.fct.2013.07.063
74. Dontu G, Abdallah WM, Foley JM, Jackson KW, Clarke MF, Kawamura MJ, Wicha MS. In vitro propagation and transcriptional profiling of human mammary stem/progenitor cells. Genes Dev 2003; 17:1253-70; PMID:12756227; http://dx.doi.org/10.1101/gad.1061803